11

X-Ray Analysis on Ceramic Materials Deposited by Sputtering and Reactive Sputtering for Sensing Applications

Rossana Gazia[1], Angelica Chiodoni[1], Edvige Celasco[2], Stefano Bianco[1] and Pietro Mandracci[2]
[1]*Center for Space Human Robotics@PoliTo, Istituto Italiano di Tecnologia*
[2]*Materials Science and Chemical Engineering Department, Politecnico di Torino*
Italy

1. Introduction

Piezoelectric materials have been extensively studied and employed over the last decades with the aim of developing new sensors and actuators to be applied in a wide range of industrial fields. The continuous increase of miniaturization requirements led also to an increasing interest in the synthesis of piezoelectric materials in the form of thin films.
As an example, the growth of wireless mobile telecommunication systems favored the expansion of the design and fabrication of high-frequency oscillators and filters (Huang et al., 2005). Within this context, conventional surface acoustic wave (SAW) filters were gradually replaced by film bulk acoustic resonator (FBAR) devices. Their advantage in comparison with SAW devices resides in a higher quality factor (Lee et al., 2003) and lower fabrication costs (Huang et al., 2005). These kinds of devices are based on piezoelectric materials. Thus, an improvement in such material properties can have a strong impact in communication performances.
A similar situation exists in the field of sensing. The increase of the sensitivity in piezoelectric sensors is one of the main targets which could be achieved by improving material characteristics.
Therefore, the interest in this class of materials is not decreasing with time. On the contrary the enhancement of the piezoelectric material performances, together with the synthesis of new lead-free piezoelectric materials and the integration of ceramic materials with flexible substrates (Akiyama et al., 2006; Wright et al., 2011), is one of the latest research goals.
Most piezoelectric materials are metal oxide and few metal nitride crystalline solids and can be single crystals or polycrystalline materials. In both cases, piezoelectric materials are anisotropic and the determination of the response of the material to an external mechanical stress induced along a certain direction on its surface must be performed along different crystallographic axes. Quantitative information about how the material responds to external stresses is given by the piezoelectric constants.
Thus, the efficiency of the piezoelectric response can strongly vary with the crystal orientation of the material, and this occurs for bulk materials and thin films (Du et al., 1999; Yue et al., 2003).

The dependence of the piezoelectric response with the crystallographic orientation makes the control of the crystal properties during the growth of thin films one of the critical points in material synthesis.
Nevertheless, also material stoichiometry control is a relevant element for the enhancement of the piezoelectric efficiency because either the presence of impurities or the lack in some of the compound constituent elements can introduce a distortion in the crystal unit cell, which may be detrimental for the piezoelectric response (Hammer et al., 1998; Ramam & Chandramouli, 2011).
In many deposition techniques the control of film stoichiometry can be a difficult task, especially for high vacuum techniques, where the presence of residual gases in the vacuum chamber can affect the final quality of the thin films.
Among them, the sputtering technique is widely used in the synthesis of piezoelectric thin films. Two approaches can be used in the growth of such materials. In the simplest, the source of material (target) is a ceramic material with the same stoichiometry as that of the desired thin film. The other approach requires the presence in the vacuum chamber of a gas able to react with the material removed from the surface of the target and form a compound while the deposition is being carried out. The main difference between the two methods is that, with the latter, a control of stoichiometry can be achieved. On the other hand, the insertion of reactive gases leads to a decrease of the sputtering rate and to target contamination. In particular, target contamination can be avoided by changing the parameters during the deposition process but, as a drawback, an increase in process complexity is introduced.
The use of characterization techniques able to give detailed information about crystal structure and chemical composition is therefore necessary in order to assess the quality of the piezoelectric thin films. Among the numerous techniques available, X-Ray Diffraction (XRD), Energy-Dispersive X-ray spectroscopy (EDX or EDS) and X-ray Photoelectron Spectroscopy (XPS) analyses can be considered exhaustive enough for the determination of such information.
Each of these characterization techniques helps in determining those film properties which are at the basis of the correct operation of the materials as piezoelectrics.
Film orientation, as previously asserted, is probably the most important characteristic regarding materials with piezoelectric properties and XRD analysis is, therefore, one of the fundamental characterization techniques to be employed for providing such information. However, materials such as ceramics tend to grow in a polycrystalline form and the evaluation of the actual orientation of the crystals can be puzzling whenever impurities and contaminations are present in the films. As an example, some peaks present in XRD spectra related to films grown by sputtering, which is a technique that can likely produce films in a crystalline form without the need of post-annealing processes, can be attributed to some crystalline phase formed by the main compound with the residual oxygen still present into the vacuum chamber at the time that the deposition is carried out. Thus, the cross-check with information supplied by compositional analysis is of fundamental importance, in order to better interpret data from XRD analysis.
In particular, EDX can help in the first qualitative evaluation of the species present in the films, while XPS can give detailed information about the nature of the bonds occurring between atoms in the films and also semiquantitative information. Thus, if the orientation of the film does not correspond to what expected, compositional analysis can provide an explanation for that, indicating whether the problem resides in the fact that the preferred

orientation of the film is different from the desired one, or in the presence of impurities in the film or in a deviation from the right stoichiometry introducing stresses in the thin film.
Aim of this work is to compare the quality of films of aluminum nitride and zinc oxide, which are piezoelectric materials, grown by sputtering and reactive sputtering in order to understand how the different approaches adopted during the deposition processes affect the film quality.

2. Sputtering growth of ceramic materials

Sputtering technique is one of the most common PVD methods used for the growth of thin films. This technique is based on the removal of atoms from the surface of a target material by using inert gas ions such as Ar ions. The atoms so obtained are able to head towards a substrate, where they can nucleate and grow as thin film. A typical sputtering system consists of an ultra-high vacuum chamber containing a target material and a substrate holder, opportunely polarized. The system is equipped with mass flow controllers, valves and gas inlets in order to create a controlled atmosphere in the vacuum chamber, which is of fundamental importance for the creation of a stable plasma. Gas plasma is generated by the voltage applied between the cathode represented by the target material and the substrate. A bias voltage could be applied when required. The ionized gas atoms or molecules present in the plasma are accelerated towards the target and are able to sputter away from its surface some atoms that afterwards are deposited on the substrate surface. There, through nucleation and coalescence processes, the atoms create a first layer of material, which is followed by the formation of additional layers, as the deposition process is carried out. During the target bombardment, secondary electrons are also emitted, allowing the plasma to be maintained (Kelly & Arnell 2000).
The target is usually composed of a metallic material or other alloys and compounds with high conductivity as well as the substrates. In fact if an insulating material is used, the DC polarization applied between target (cathode) and substrate (anode) in a sputtering system induces a charge accumulation able to slowly reduce the ions acceleration towards the target, with the creation of an electric field in opposition to that generated by the DC polarization. For this reason it turns out to be necessary to modify the set up for the deposition of insulating materials. The application of a high frequency voltage can overcome the problem of charge accumulation, and this solution is found in RF sputtering systems. The typical voltage frequency for a standard RF sputtering system is 13.56 MHz. Such solution allows for the deposition of oxides, nitrides and other insulating materials on both metallic and insulating substrates.
The sputtering rate associated to each material depends on numerous parameters, including the sputtering efficiency of the gas which is strictly related to the mass of the gas atoms. For this reason gases with heavy atoms are preferred and argon is the most common gas used in sputtering processes. However, when compounds are to be obtained by sputtering, reactive gases are used, such as oxygen or nitrogen. Because of the role played by these gases during a thin film deposition, they are named “sputtering gases”.
In a sputtering process the gas is inserted in the vacuum chamber only after a very low pressure (of the order of 10^{-5} Pa) has been reached. At these pressure levels, most of the contaminant species that could alter the film final composition are not present anymore, with some exceptions, and in principle the sole gas participating to the growth process is the one deliberately inserted in the vacuum chamber. In order to achieve low pressure values

two kinds of vacuum pumps are required: one for the rough vacuum and one for the high vacuum. Typically, a rotary pump and a turbomolecular pump are employed for reaching high vacuum regime in a sputtering system. Rotary pumps usually allow to reach pressures of about 10^{-1} Pa while, with turbomolecular pumps, pressures down to 10^{-5} Pa can be achieved.

When the gas is inserted in the vacuum chamber at the desired flow, and the gas pressure is set to the value fixed for the deposition process, the plasma can be generated between the two electrodes present in the system. The target material is actually one of the two electrodes (the cathode). To provide a compensation for the local temperature increase caused by the energy transfer from the incident ions to the target surface, and during the high temperature processes, the cathode is usually equipped with a cooling system. The substrate is placed at the anode. This is the simplest sputtering system configuration, the so-called diode sputtering (Wasa et al., 2004a) and can be used with both DC and RF power supply. In order to increase the sputtering efficiency, a system of magnets with an appropriate configuration can be adopted. This system is intended to create a magnetic field parallel to the target surface that, affecting the trajectory of the secondary electrons, is able to confine them in proximity of the target surface, increasing the probability of collision between electrons and gas atoms and consequently of their ionization (Kelly & Arnell 2000). This region of denser plasma increases the sputtering rate of the target material. This modified system is called magnetron sputtering (Wasa et al., 2004b).

2.1 Sputtering growth of ceramic materials in reactive mode

The reactive sputtering technique is similar to the classic sputtering technique in all aspects, with one exception, that is the type of gas inserted in the vacuum system. In section 2, argon is indicated as the gas usually employed in a sputtering deposition process. However, for reasons that will be explained later in this section, it is necessary sometimes to be able to vary the stoichiometry of a compound to be grown in the form of thin film. In such cases, what is called a 'reactive gas' must be inserted in addition or in substitution of the sputtering inert gas. If the latter condition occurs, the gas is at the same time named sputtering and reactive gas.

At the base pressure reached with conventional vacuum systems, almost all those species that could alter the desired stoichiometry of a thin film are absent. However, in real systems there is always some residual unwanted gases that participate in the reaction between the target material and the reactive gas (Sproul et al., 2005). As previously asserted, the most commonly used reactive gases are oxygen and nitrogen, the former being used in oxide depositions, the latter in nitrides formation. In both cases, the target is usually a metallic material that reacts with the ionized gas atoms or molecules, generated by plasma, after its transition into vapor phase. The reason for using this approach is that it allows the control of the stoichiometry of the films formed on the substrate material. Although targets made of stoichiometric compounds are commercially available, sometimes it is required to adjust the stoichiometry of the films in order to gradually change their properties. By regulating the gas flow in the chamber or the concentration of the reactive gas in a mixture of sputtering and reactive gases, it is possible to regulate also the percentage of gas atoms or molecules bound to the metal ions.

The most important drawback in such a process is the phenomenon of the so-called target poisoning. It basically consists of the contamination of the target surface with the compound

formed by the reaction between gas molecules and target atoms (Sproul et al., 2005), while in solid phase. When the target surface is totally covered by this compound, the target is poisoned (Sproul et al., 2005). Many works (Berg & Nyberg, 2005; Maniv & Westwood, 1980; Safi, 2000; Sproul et al., 2005; Waite & Shah, 2007) reported on the dependence on the reactive gas flow of both the target poisoning effect and the sputtering rate of the target material. Sputtering rates from compound targets are lower than that of pure metallic targets mainly because the sputtering yield of metal atoms from a compound on the target surface is lower than that from a pure metallic target. The ideal working point in terms of gas flow should be in between the elemental region (i.e., where the target is not contaminated at all), and the condition of target poisoning, but this region is not very stable and even weak variations of the growth conditions can lead to target poisoning (Sproul et al., 2005). Thus, it is very often necessary to work at low deposition rate and not having a full control of the stoichiometry of the thin films. The phenomenon of target poisoning described above occurs only when cathodes having uniform plasma density at their surface are used. In the case of magnetron cathodes, the formation of a compound at the target surface is position-dependent due to the low spatial homogenity of the magnetic field, and there is the possibility of the contemporary presence of three states across the surface: metallic, oxidized and partially oxidized (Safi, 2000). Many solutions for the process stabilization have been proposed, based on the variation of different parameters, such as pump speed or gas flow inserted into the vacuum chamber (Safi, 2000; Sproul et al., 2005).

3. Growth of piezoelectric ceramic materials on silicon substrates

The sputtering system used for depositing the films herein described and analyzed includes a stainless steel cylindrical reactor containing a magnetron sputtering source, capable of carrying a target of 10 cm in diameter. The source is fixed at the upper part of the reactor, facing downwards, whilst the silicon substrates are placed at the bottom part of the reactor, facing upwards, at a distance of 80 mm from the sputtering target. The system is pumped both by a turbomolecular pump and a mechanical pump in sequence (nominal pumping speeds 350 l/s and 15 m^3/h respectively). The gases employed during the growth processes are injected into the reactor by means of mass flow controllers and the plasma discharge is lit by applying a radio frequency voltage at a frequency of 13.56 MHz between the target and the grounded substrate holder. The plasma impedance is then tuned by a matching network to reduce reflected power down to negligible values.
Before each deposition process the silicon substrates were cleaned in an ultrasonic bath with acetone (10 min) and ethanol (10 min) and dried under direct nitrogen flow. The substrates were then placed inside the vacuum chamber, which was evacuated down to a pressure of about 10^{-5} Pa.

3.1 Growth of ZnO thin films

Zinc oxide thin films were grown on [100]-oriented silicon substrates at room temperature, i.e., no intentional heating was applied to the substrates. Two different targets were used for the deposition processes: a Zn target (Goodfellow, purity 99.99+%) and a ZnO target (Goodfellow, purity 99.99%). The films were deposited according to three different approaches exploiting the two targets and different gas mixtures. In particular the films were grown by:

- sputtering the Zn target in a mixture of Ar and O_2
- sputtering the ZnO target in Ar atmosphere
- sputtering the ZnO target in a mixture of Ar and O_2

Two of the three approaches involve the reactive sputtering mode, while the other method avoids the use of a reactive gas, and the only source of oxygen should be the target itself. The complete sets of process parameters are reported in Table 1.

Sample Name	Target	Base pressure	Ar flow	O_2 flow	Pressure	Power	Deposition time	Thickness
		(Pa)	(sccm)	(sccm)	(Pa)	(W)	(min)	(nm)
ZnO_MR	Zn	5.3E-05	39	1	0.67	100	60	220
ZnO_CN	ZnO	1.6E-05	40	-	0.67	100	120	210
ZnO_CR	ZnO	2.9E-05	40	1	0.67	100	120	200

Table 1. Deposition conditions for the growth of ZnO thin films

The name of each sample reports the name of the material and two letters representing the nature of the target (Metallic, Ceramic) and the sputtering mode (Reactive, Non-reactive). The deposition time was chosen on the basis of a previous optimization work performed on the conditions of depositions of each class of films.

3.2 Growth of AlN thin films

Aluminum nitride thin films were grown on [100]-oriented silicon substrates at room temperature. Two different targets were used for the deposition processes: an Al target (Goodfellow, purity 99.999%) and an AlN target (Goodfellow, purity 99.5%). As for ZnO films, AlN films were deposited according to three different approaches involving the two targets and different gas mixtures. In particular the films were grown by:

- sputtering the Al target in N_2 atmosphere
- sputtering the AlN target in Ar atmosphere
- sputtering the AlN target in a mixture of Ar and N_2

The complete sets of process parameters are reported in Table 2.

Sample Name	Target	Base pressure	Ar flow	N_2 flow	Pressure	Power	Deposition time	Thickness
		(Pa)	(sccm)	(sccm)	(Pa)	(W)	(min)	(nm)
AlN_MR	Al	4.0E-05	-	40	0.35	100	180	210
AlN_CN	AlN	1.6E-05	40	-	0.67	100	120	60
AlN_CR	AlN	2.9E-05	40	1	0.67	100	120	55

Table 2. Deposition conditions for the growth of AlN thin films

For the names of the samples, the same criterion exposed in section 3.1 was applied. As well as in the case of ZnO thin films, the sputtering time and the gas pressure used for the growth of sample AlN_MR were chosen on the basis of the characterization results obtained from previous depositions of AlN films.

4. X-Ray analysis on ceramic thin films

PVD techniques usually allow the growth of thin films having the same stoichiometry of the source of material used during the deposition process. However, in the case of growth of compound thin films, the conditions in which the growth processes occur can cause either lacks of some of the elements making part of the compound, or contamination with other undesired elements. In other words, a key role is played by the deposition conditions in the growth process of a thin film with the correct stoichiometry.

The concentration of elements, and the way they are bound to each other, affects also the physical properties of materials. For this reason, chemical composition analysis is of fundamental importance since it helps to optimize those process parameters which directly influence the chemical composition of materials in order to obtain high-quality thin films, with optimum properties.

Energy Dispersive X-ray spectroscopy is a powerful technique for the investigation of the chemical species present in a material. It is based on the analysis of the energy and intensity distribution of the x-ray signal generated by the interaction of an electron beam with a specimen (Goldstein et al., 2003a). EDX is an optional tool installed on electron microscopes. In such a set up an electron beam is directed towards the sample to be analyzed. The electrons with a certain kinetic energy can interact with the nucleus or with the electrons of a specific atom. The Coulombic interaction with the positive nucleus causes a deceleration that is responsible for an energy loss, the so called bremsstrahlung radiation (Goldstein et al., 2003b). Since the electrons may lose any amount of energy between zero and the initial energy, the detection of this emitted radiation gives rise to a continuous electromagnetic spectrum that constitutes the background of the collected spectrum (Goldstein et al., 2003a). When the primary electrons interact with the electrons of the atom, ionization phenomena occur, usually involving K shell electrons. Since the atom in this excited state tends to reach the minimum of energy, the electrons from L or M shells can occupy the vacancy left from the K shell electron. The transition between L and K or M and K shells cause an emission of X-ray radiation designated as K_α and K_β, respectively (Goldstein et al., 2003c). The energy difference between L, M and K levels are well defined for each element, so the emission of K_α and K_β X-rays identifies the elements present in the analyzed sample. The detection of this transition levels should in principle give a line in the continuous electromagnetic spectrum. However, the typical peak width of an EDX spectrum is about 70 times wider than the natural line width (Goldstein et al., 2003d). The spatial resolution of this technique is strictly related to the region of the sample interacting with the electron beam that is the X-ray generation volume. In fact, this volume depends on the material density and on the critical ionization energy, i.e., the energy that the primary electron beam should have in order to ionize atoms of the specimen (Goldstein et al., 2003e).

Both the depth and the lateral distribution of the X-ray production is relevant because in depth it determines the amount of photoelectric absorption of X-rays from the material atoms, and laterally it determines the spatial resolution of the X-ray microanalysis. However, the photoelectric absorption phenomenon is not significant in micron-sized samples so this side effect can be ignored (Goldstein et al., 2003e).

A fundamental aspect of this technique is the X-ray detection. It is usually performed using solid state detectors, especially lithium-drifted silicon detectors. The detection range is comprised between 0,2 and 30 KeV (Goldstein et al., 2003f). EDS analysis on ZnO and AlN

thin films were performed with an Oxford INCA Energy 450 installed on a Field Emission Scanning Electron Microscope SUPRA 40 (ZEISS).

X-ray Photoelectron Spectroscopy is an advanced technique for the study of the surface composition of a wide range of materials, stated that they have to be vacuum-compatible. The sampling depth, defined as the depth from which 95% of all photoelectrons are scattered by the time they reach the surface, ranges between 5 and 10 nm below the surface. The phenomenon at the basis of this technique is the photoelectron emission that involves energy exchanges between a source of x-rays and a specimen, according to the following equation (Briggs, 1983):

$$E_K = h\nu - E_B - \phi \tag{1}$$

where E_K is the measured electron kinetic energy, $h\nu$ the energy of the exciting radiation, E_B the binding energy of the electron in the specimen, and ϕ the work function, the latter having a specific value depending on the material and on the spectrometer (Briggs, 1983a). As stated above, the exciting radiation is derived from an X-ray source. The material responsible for the emission of X-rays must be chosen taking into account two aspects: the X-ray line width cannot exceed a certain value that otherwise would strongly limit the resolution of the measurement, and the energy associated to the X-ray must be high enough to allow the ejection of a sufficient range of core electrons for unambiguous analysis (Briggs, 1983b). Usually K_α radiation from aluminum or magnesium is employed to excite the material atoms. Photoelectron energy is measured by an appropriate analyzer. Many types of analyzers have been proposed over the last decades, although the simplest and most common ones are the cylindrical mirror analyzer (CMA) and the concentric hemispherical analyzer (CHA) (Briggs, 1983c). The energy associated to the photoemitted electrons precisely identifies a material. Since this energy varies with respect to the shell the electron is ejected from, each peak in the spectrum will correspond to the energy associated to the electrons ejected from all those levels that require an excitation energy lower than that of the incident X-rays. If the specimen is a compound material, each peak will represent the energy associated to the photoelectrons from all the elements present in that compound. However, peaks corresponding to the same element undergo what is called a chemical shift if the boundary conditions of the element change, i.e., the energy associated to photoelectrons ejected from an atom of an element changes with the molecular environment, with the oxidation state, or with its lattice site (Briggs, 1983d). Chemical shifts allow to understand how atoms are bound within compounds and alloys. Aluminum nitride and zinc oxide thin films were characterized with XPS technique in order to determine their exact chemical composition. The instrument used for XPS analysis was a PHI 5000 VersaProbe Scanning ESCA microprobe - Physical Electronics, equipped with an ion gun used in these experiments for cleaning the surface before each measurement, in order to remove any impurity from the analyzed area. A dual beam charge neutralization method was employed during the measurements, in order to reduce the charging effect on the samples. This charge neutralization method consists in a combination of low energy argon ions and electrons.

X-Ray Diffraction technique is employed for the analysis of the crystallographic properties of materials. The diffraction method is based on the following equation:

$$\lambda = 2d_{hkl}\sin\theta \tag{2}$$

the well known Bragg law, where λ is the x-ray wavelength which irradiates the sample to be analyzed, d_{hkl} is the lattice spacing of a specific (hkl) family planes of the crystalline material, and θ is the diffraction angle of the X-ray beam with respect to the direction parallel to the (hkl) plane. For a given (hkl) family, characterized by a precise value of d_{hkl}, the conditions on λ and θ are then very stringent. According to this equation, in a crystal it is possible to observe diffracted beams only along fixed directions, determined by the constructive interference between diffracted beams at the different crystal planes. Each single atom is actually able to scatter an incident beam of X-rays along every direction, but a periodic arrangement of atoms cancels, with a destructive interference phenomenon, all those beams scattered along the directions not satisfying equation (2). The analysis of materials with unknown values of lattice spacing is carried out by varying either the incidence angle or the wavelength of the X-ray beam. Depending on which of the two parameters is varied, the diffraction methods are named as follows (Cullity, 1956a):

- Laue method, where λ is varied and θ fixed;
- Rotating-crystal method, used for monocrystals only, where λ is fixed and the crystal rotates;
- Powder method, where λ is fixed and θ is varied.

The latter has been used for the characterization of all the samples described in the next chapters, although thin films were not reduced in powder.

The instrument used to perform XRD measurements is called diffractometer, and it consists of a monochromatic X-ray source and an X-ray detector (commonly named counter), both placed on the circumference of a circle having its centre on the specimen. The specimen is held by an appropriate holder, placed on a table which can rotate about its axis, which is also the axis about which X-ray source and detector are able to rotate. X-rays are sent to the specimen where they are diffracted to form a convergent beam focused on a slit placed just before the X-ray detector.

A filter is also placed in the diffracted beam path in order to suppress K_β radiation. The counter position can be read on a graduated scale of the goniometer and it corresponds to 2θ. Moreover the table where the specimen holder is fixed and the counter are mechanically coupled in a way that a rotation of the specimen of x degrees corresponds to a rotation of the counter of $2x$ degrees (Cullity, 1956b). The values of the parameter θ correspond to the angular positions where peaks of diffracted X-ray intensity are registered. After the whole set of values for θ is determined, lattice spacings d_{hkl} corresponding to different crystal planes can be calculated. Lattice spacing, however, is not the only parameter that can be obtained from an XRD measurement. The evaluation of the crystals size (t) is strictly related to the structural properties of materials, (Cullity, 1956c) and can be calculated as follows:

$$t = \frac{0.9\lambda}{B\cos\theta_B} \tag{3}$$

where λ is the X-ray wavelength, B is the peak width in radians, measured at the half the maximum intensity, and θ_B is the angle satisfying equation (2). Equation (3) is known as the Scherrer formula (Cullity, 1956d). Because of its formulation, equation (3) does not take into account the role of strain in the material.

The instrument used for the characterization of AlN and ZnO films was a Panalytical X'Pert MRD PRO diffractometer, equipped with a Cu K_α radiation source (λ = 1.54056 Å).

4.1 X-Ray analysis on ZnO thin films

ZnO was extensively studied over the last decades with the aim of producing high-quality thin films for the fabrication of SAW and FBAR devices (Ferblantier et al., 2005; Huang et al., 2005; Lee et al., 2003). These kinds of devices exploit the piezoelectric properties of their active layers. Materials exhibiting high piezoelectric coupling factor are usually highly oriented along one axis. For ZnO the *c*-axis orientation presents the highest piezoelectric coefficient and for this reason many works, more or less recent (Muthukumar et al., 2001; Sundaram et al., 1997; Yan et al., 2007), focused their attention on the XRD analysis and electrical characterization of the piezoelectric layers, often neglecting the analysis of the film composition. The lack of one of the elements in the film can be detrimental in the final response of the material when used in the fabrication of piezoelectric devices. For this reason it is crucial to grow highly oriented and highly stoichiometric materials for optimizing their piezoelectric properties. Moreover, techniques such as sputtering require very long optimization processes in order to satisfy the two requirements.
The combination of the results obtained from the X-ray analyses performed on the films described in this work will show how important is to combine the information collected by different techniques in order to precisely evaluate and improve the material properties.

4.1.1 EDS analysis on ZnO thin films

A first evaluation of the composition of the ZnO thin films grown by the three different approaches described in section 3.1 was assessed by EDS analysis. The system for the microanalysis was first calibrated with a Co sample, used as reference material to check the performance of the instrument. The spectra reported in Figure 1 refer to the whole area of the FESEM images shown below. All the spectra were collected by using the same conditions (electron energy, magnification, integration time).
The spectra were analyzed in standardless mode and the related semiquantitative information about the elements and their concentration is reported in Table 3. Four elements were detected. The Si peak is related to the substrate contribution, the C peak is related to organic impurities on the surface of the sample. The Zn peak is obviously related to zinc oxide, while the oxygen peak is partially related to this oxide.

Element	C K	O K	Si K	Zn K
	Atomic concentration (%)	Atomic concentration (%)	Atomic concentration (%)	Atomic concentration (%)
ZnO_MR	6.79	31.28	45.97	15.97
ZnO_CN	5.90	31.35	46.72	16.03
ZnO_CR	5.31	30.00	49.96	14.73

Table 3. Atomic percentages of the elements detected by EDS analysis on the ZnO thin films

The excess of oxygen with respect to the desired stoichiometry of the films can be attributed to the fact that silicon is bound to oxygen, creating an oxide phase at the interface between the substrate and the film. However, since the oxygen peak area is the result of the contributions of the oxygen in the zinc oxide film and the oxygen present in the native silicon oxide layer present at the substrate surface, it is not possible to precisely determine

the amount of oxygen actually bound to zinc in the compound. With the exception of carbon, usually present on the surface of materials exposed to air, no element different from the expected ones was detected with EDS analysis. A more precise evaluation of the film composition must be supplied with the help of other techniques.

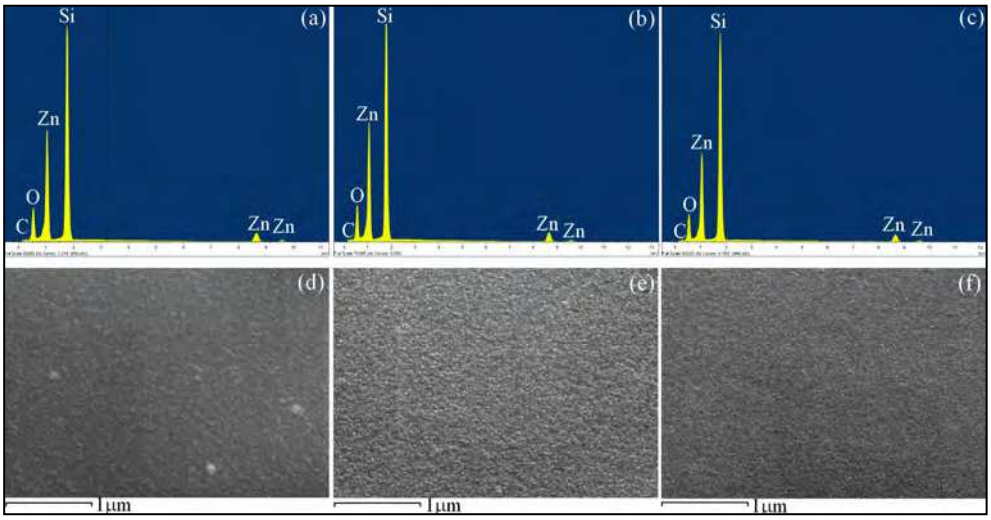

Fig. 1. EDX spectra and FESEM images of ZnO thin films grown from metal target (a, d), ceramic target in Ar atmosphere (b, e) and ceramic target in a mixture of Ar and O_2 (c, f).

4.1.2 XPS analysis on ZnO thin films

The XPS technique can give precise information about the composition of the first atomic layers of a material. This capability is of fundamental importance when dealing with applications where the study and control of surface properties is crucial. In the present case, instead, the desired information is not related to the actual surface composition: the piezoelectric constants of the materials are not related to the surface composition but to the crystallographic orientation of grains with the right stoichiometry. The exposure of the samples to air promotes the contamination of the surfaces (as shown from the EDX spectra reported above). As a result, the elements present on the sample surface are not the same that constitute the overall material layer. For this reason, in order to obtain information about the composition of the whole film, the removal of surface contamination before the acquisition of each XPS spectrum is mandatory and is usually performed by sputtering the surface with argon ions. The contamination of surfaces (adventitious carbon) due to exposure to air mainly generates C-C and C-H bonds. Carbon peak C1s is commonly used as a reference for the compensation of the XPS spectrum shift caused by the charge accumulation effect due to the charged particles reaching the sample surface during the analysis. However after the removal of all the surface contaminations the carbon peak is not detectable anymore since no source of this element is present during the film growth process. On the basis of these considerations, XPS spectra were acquired before and after the surface cleaning. With a high resolution acquisition before the surface cleaning the C1s peak position was precisely determined. The second high resolution acquisition determined the

position of the peaks related to each constituent element in the film. The difference between the energy the C1s peak is centered at and the energy the carbon peak from database is centered at (fixed at 284.6 eV) gives the shift to be applied to all the acquired peaks in the XPS spectrum. This procedure was applied to all the samples herein described. For the determination of the exact peak positions all the peaks were fitted with a Gaussian-Lorentzian function. The concentration of the elements in the film was calculated by the MultiPak v.9.0 software according to the following equations:

$$\text{Oxygen concentration (\%)} = \frac{A_O \times SF_O}{\left(A_O \times SF_O\right) + \left(A_{Zn} \times SF_{Zn}\right)} \times 100 \quad (4)$$

$$\text{Zinc concentration (\%)} = \frac{A_{Zn} \times SF_{Zn}}{\left(A_O \times SF_O\right) + \left(A_{Zn} \times SF_{Zn}\right)} \times 100 \quad (5)$$

where A_O and A_{Zn} are the areas of the O1s and Zn2p$^{3/2}$ peaks, respectively, and SF_O and SF_{Zn} are the sensitivity factors for oxygen and zinc, respectively. Figure 2 shows the O1s and Zn2p$^{3/2}$ peaks acquired with the post-cleaning high-resolution analysis on the ZnO_MR sample.

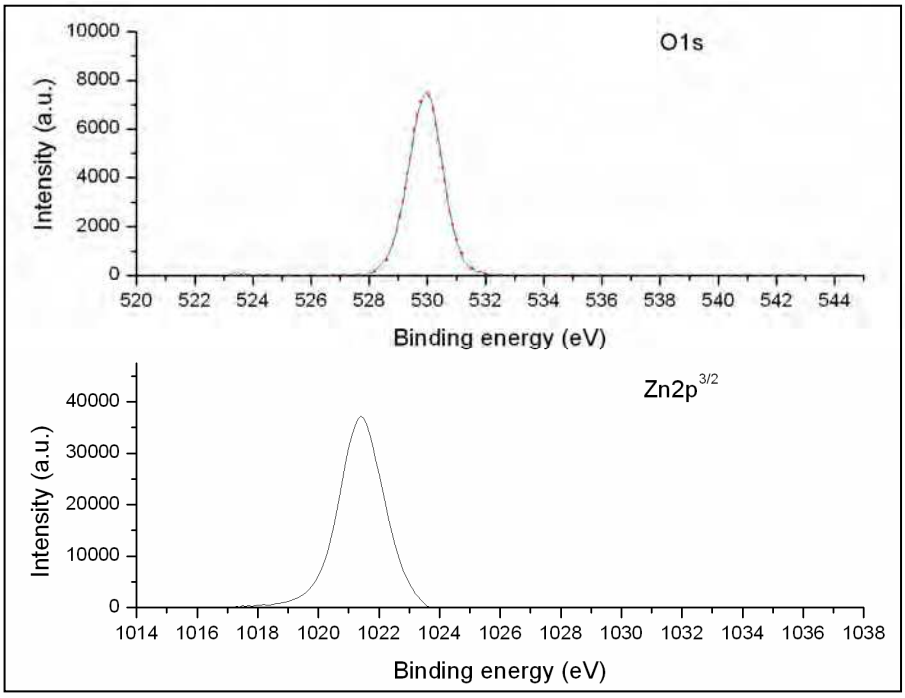

Fig. 2. O1s and Zn2p$^{3/2}$ XPS peaks acquired after surface cleaning on ZnO_MR sample. The dotted red line represents the peak fitting the O1s peak.

The O1s peak is centered at 529.9 eV, the typical position of the oxygen peak in Zn-O bonds (Haber et al., 1976). The calculated concentrations are reported in Table 4. The excess of Zn with respect to oxygen reveals that the film contains also Zn-Zn bonds. In order to evaluate the percentage of such bonds, the zinc peak should be fitted with two appropriate curves. The areas of the fitting curves centered at the typical binding energies of Zn in the Zn-Zn and Zn-O bonds represent the percentages of the metallic phase and the oxide phase. Unfortunately these binding energies are 1021.5 eV and 1021.7 eV, respectively (Klein & Hercules, 1983), and are too close to univocally fit the $Zn2p^{3/2}$ peak. However, for the absence of any other contaminant in the film, it is reasonable to assert that the overall Zn excess constitutes a metallic zinc phase in the film.

Figure 3 reports the high resolution peaks of ZnO_CN sample. Again it is not possible to precisely determine the metallic phase percentage by fitting the peaks revealed during the analysis. However, again in this case, the amount of impurities can be neglected. The carbon concentration is very low indeed (Table 4) and there is no evidence that a consistent portion of it could be bound to oxygen atoms. The peaks fitting the O1s peak and centered at 529.7 eV, 531.6 eV and 532.3 eV can be in fact identified with the binding energies of O-Zn bonds (Chen et al., 2000), O-H bonds and oxygen bound in the H_2O molecule, respectively (Avalle et al., 1992). The latter is present in particular because of the possible presence of humidity inside the vacuum chamber which is not equipped with a load-lock chamber and requires to be opened every time a substrate has to be loaded for a new process.

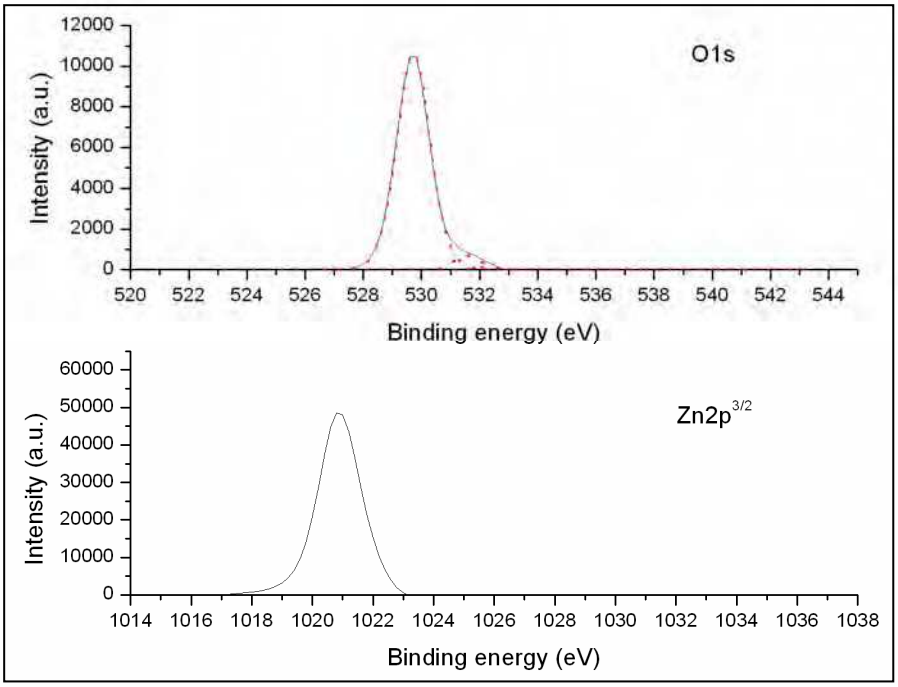

Fig. 3. O1s and $Zn2p^{3/2}$ XPS peaks acquired after surface cleaning on ZnO_CN sample. The dotted red lines represent the peaks fitting the O1s peak.

However the total area of the two peaks related to the binding energy of oxygen bound to hydrogen atoms is less than the 7% of the total O1s peak area. This means that the 93% of oxygen atoms are bound to zinc. The Zn excess produces a metallic phase in the film as for ZnO_MR sample. Although the target used for the growth of sample ZnO_CN is stoichiometric, the film presents a lack of oxygen which needs to be compensated.
In the case of ZnO_CR sample, grown in a mixture of Ar and O_2, there was still an excess of zinc (see Table 4). However the concentration of oxygen in the gas mixture was very low (1 sccm over a total flow of 41 sccm) and probably the amount of gas required to obtain the right stoichiometry should be higher. High resolution peaks for ZnO_CR sample are reported in Figure 4. Zinc peak was not fitted because of the impossibility to exactly determine the position of the two peaks representing the binding energies associated to Zn-O and Zn-Zn bonds. The O1s peak was fitted with two curves, one centered at 529.7 eV (O-Zn bonds), and the other centered at 531.7 eV (O-H bonds), very close to those chosen for fitting the O1s peak in the XPS spectrum of ZnO_CN sample. The amount of contamination due to the humidity present in the chamber is basically the same as that of ZnO_CN. It is identified by the small peak on the right-bottom part of the O1s peak shown in Figure 4, with a peak area of about the 4% of the total O1s peak area.

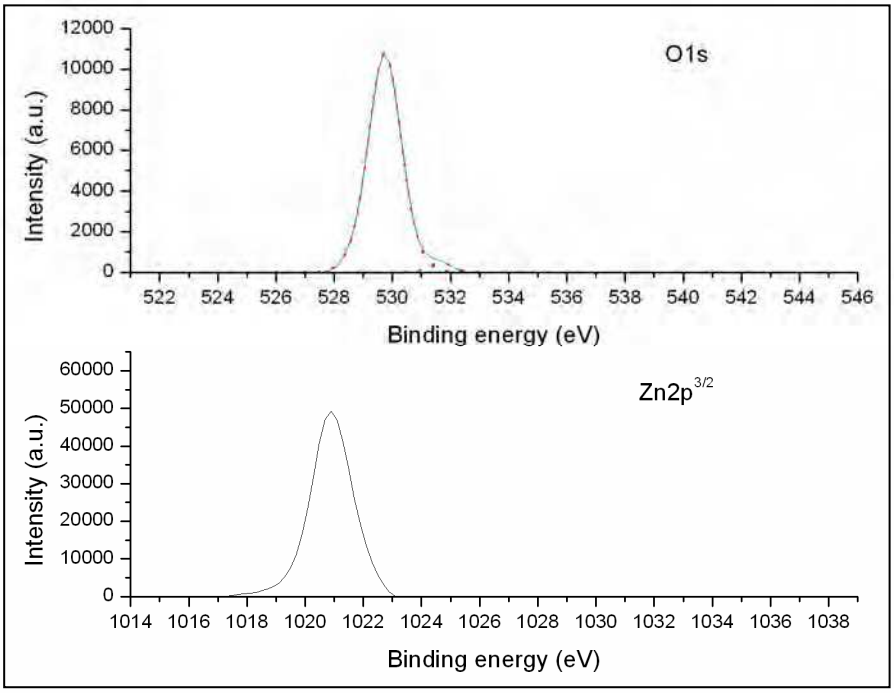

Fig. 4. O1s and $Zn2p^{3/2}$ XPS peaks acquired after surface cleaning on ZnO_CR sample. The dotted red lines represent the peaks fitting the O1s peak.

Sample name	C atomic concentration	O atomic concentration	Zn atomic concentration
	(%)	(%)	(%)
ZnO_MR	-	40.9	59.1
ZnO_CN	0.7	44.0	55.3
ZnO_CR	-	43.9	56.1

Table 4. Atomic concentrations obtained by fitting the O1s and $Zn2p^{3/2}$ peaks from the XPS spectra of ZnO thin films

4.1.3 XRD analysis on ZnO thin films

XRD analysis on ZnO thin films was carried out in order to assess the crystallographic orientation of the material since from this information it is possible to predict how efficient the material will be in terms of piezoelectric response. XRD spectra acquired on ZnO are shown in Figure 5 and the peak positions are reported in Table 5. The peak positions were determined by fitting the spectra with Pseudovoigt curves.

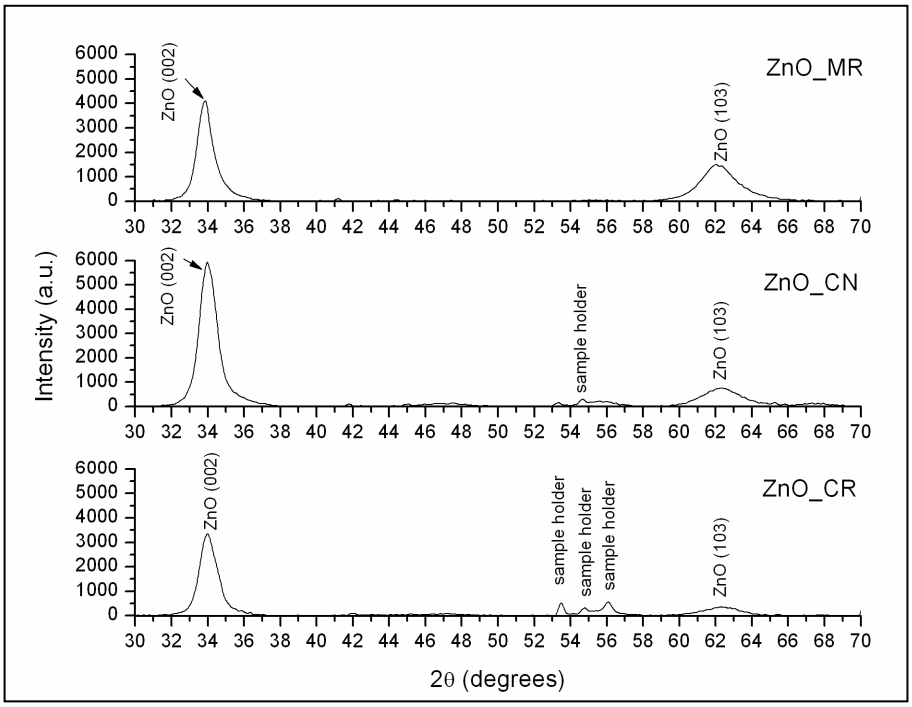

Fig. 5. XRD patterns of ZnO thin films

Two main peaks were identified in the XRD patterns of all the three samples, one related to the [002] orientation and one to the [103] orientation of ZnO. Peaks detected in the ZnO_MR

sample are the most shifted with respect to the database peak positions (JCPDS, 1998a). These data are in agreement with the fact that the metallic phase in this film was the largest in comparison with the other samples. The presence of a high amount of metallic phase might have induced a tensile stress in the zinc oxide unit cells with the effect of producing a shift towards lower angle values. To this end it is worth to notice that no peak related to any zinc crystallographic orientation was detected. Thus we can consider the metallic zinc as an impurity instead of a single phase.

For what concerns the peak relative intensities, the [002] peak intensity of sample ZnO_CR is about 10 times higher than the [103] peak intensity, meaning that during the growth from ceramic target the presence of oxygen favors the growth of crystals along the [002] orientation.

The ratio between the intensities of the two peaks in sample ZnO_CN was in fact lower (about 8). The sample grown from the metal target (ZnO_MR) showed the lowest intensity ratio (about 3).

It can be concluded that, on the basis of the whole set of results, ZnO_CR sample could in principle perform better than the other samples in terms of piezoelectric properties.

Sample name	Peak position (2θ)	
	ZnO [002]	ZnO [103]
	(degrees)	(degrees)
Database (JCPDS, 1998a)	34.379±0.001	62.777±0.001
ZnO_MR	33.86±0.02	62.17±0.02
ZnO_CN	34.03±0.02	62.33±0.02
ZnO_CR	34.03±0.02	62.22±0.02

Table 5. Position of the peaks detected during XRD analysis performed on ZnO thin film

4.2 X-Ray analysis on AlN thin films

Aluminum nitride is a semiconductor of the III-V semiconductor group, with an hexagonal wurtzite crystalline structure (Penza et al., 1995; Xu et al., 2001), lattice constants of a = 0.3110 nm e c =0.4980 nm (Xu et al., 2001), and is characterized by a broad direct energy gap (6.2 eV) (Cheng et al., 2003; Hirata et al., 2007; Penza et al., 1995), chemical stability (Cheng et al., 2003; Penza et al., 1995), high thermal conductivity (3.2 W/mK) (Cheng et al., 2003), low thermal expansion coefficient (4.5 ppm/°C) (Ruffner et al., 1999), high breakdown voltage (Hirata et al., 2007; Xu et al., 2001), high acoustic speed (Cheng et al., 2003; Xu et al., 2001), high refractive index (n = 2.1) (Penza et al., 1995), high electrical resistivity (10^{11}-10^{14} Ωcm) (Ruffner et al., 1999) and, above all, good piezoelectric response (Cheng et al., 2003; Hirata et al., 2007; Penza et al., 1995; Ruffner et al., 1999; Xu et al., 2001) (piezoelectric coefficient of 5.4 pm/V) (Ruffner et al., 1999). Piezoelectric behaviour of AlN strongly depends on its crystallographic orientation (Cheng et al., 2003) and, in particular, films grown in the [002] orientation are preferred as the highest

piezoelectric stress constant is associated to this orientation (Cheng et al., 2003). Piezoelectricity in AlN has been demonstrated only when in the form of a thin film (Gautschi, 2002). Analysis performed by many research groups on reactive-sputtered AlN films (Cheng et al., 2003; Penza et al., 1995; Xu et al., 2001) revealed the strong dependence of film crystal orientation on growth parameters, such as target-substrate distance, power applied to the target, substrate temperature, process pressure, and gas relative concentration when a mixture of Ar and N_2 was employed for the depositions of AlN. An interesting advantage of growing AlN by reactive sputtering is the possibility to obtain polycrystalline films at low substrate temperatures (from room temperature up to ˜200 °C (Penza et al., 1995; Xu et al., 2001).
As for ZnO, AlN thin films were characterized by EDS, XPS and XRD techniques, in order to assess the film quality and to find out relationships between film properties and growth conditions.

4.2.1 EDS analysis on AlN thin films

EDX spectra and FESEM images obtained from the analysis of AlN thin films, deposited with the three different approaches described in section 3.2, are shown in Figure 6. The results from microanalysis are reported in Table 6.

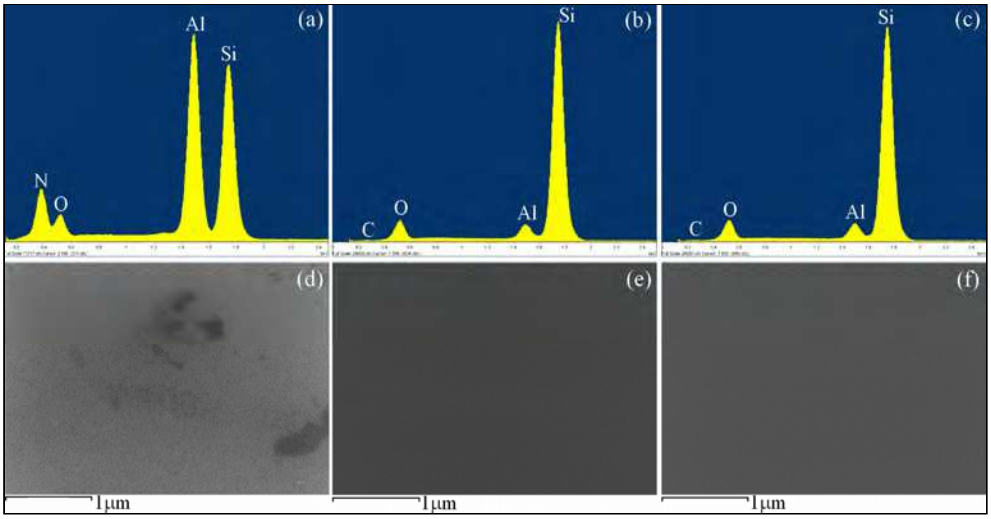

Fig. 6. EDX spectra and FESEM images of AlN thin films grown from metal target (a, d), ceramic target in Ar atmosphere (b, e) and ceramic target in a mixture of Ar and N_2 (c, f).

The information acquired with this kind of analysis is of fundamental importance for the interpretation of the results obtained from the other analysis performed on the AlN samples. It can be observed indeed that the nitrogen peak was not detected in any of the films deposited from ceramic target, while it is present in the spectrum of the sample grown from a metallic aluminum target in nitrogen atmosphere. Also in this case the data acquired with the EDS technique are not enough to assert that AlN_CN and AlN_CR samples do not

contain nitrogen. A relevant issue for the energy-dispersive X-Ray spectroscopy technique is that release of volatile elements (such as nitrogen) can occur during the analysis (Bohne et al., 2004). Thus, in samples characterized by low nitrogen concentration the detection of the nitrogen peak can be difficult.
In the case of the two samples grown from ceramic target only aluminum and oxygen were detected (as well as the silicon peak from the substrate and carbon traces as impurities).
For what concerns the film grown from a metal target, nitrogen and oxygen peaks are strong enough to be clearly distinguished. Oxygen peak detected on the sample comprises the contribution of the signals generated by the oxygen contained in the film and by the oxygen contained in the layer of native oxide present on the silicon substrate, and it is not possible to estimate which is the percentage of each contribution for the two layers (Bohne et al., 2004). In consideration of the limit of this characterization further analysis are required in order to better evaluate the composition of each film.

Element	N K	C K	O K	Al K	Si K
	Atomic concentration (%)	Atomic concentration (%)	Atomic concentration (%)	Atomic concentration (%)	Atomic concentration (%)
AlN_MR	38.76	-	9.72	24.11	27.40
AlN_CN	-	2.17	16.32	3.91	77.60
AlN_CR	-	2.50	16.83	4.20	76.47

Table 6. Atomic percentages of the elements detected by EDS analysis on the AlN thin films

4.2.2 XPS analysis on AlN thin films

AlN samples were treated with the same surface cleaning process as ZnO samples (see section 4.1.2). XPS spectra acquired on sample AlN_MR confirmed the presence of nitrogen found by means of the EDS analysis. The peaks of the elements present in the film are shown in Figure 7, while the values of elemental concentration obtained for all the AlN samples are reported in Table 7. If qualitative information is basically the same for the two techniques, with the exception of the presence of the silicon peak that is not found in the XPS spectrum for the intrinsic properties of such a technique, quantitative information are different. By comparing the values reported in Table 6 and Table 7 it is evident that the concentrations of each element are strongly different. For what concerns the oxygen concentration, which results to be much higher from the XPS analysis than from EDS analysis, it has to be noticed that the surface of the material can contain a higher amount of this element if compared with bulk because of the capability of the surface to be oxidized. In principle, the oxygen concentration calculated from EDX spectra could be more accurate when considering the whole film volume composition. On the other hand the surface cleaning process performed just before the XPS analysis should have prevented from the analysis of the very first layers of the sample which could have undergone a higher oxidation with respect to deeper layers. For this reason information from the XPS analysis are expected to be more reliable.

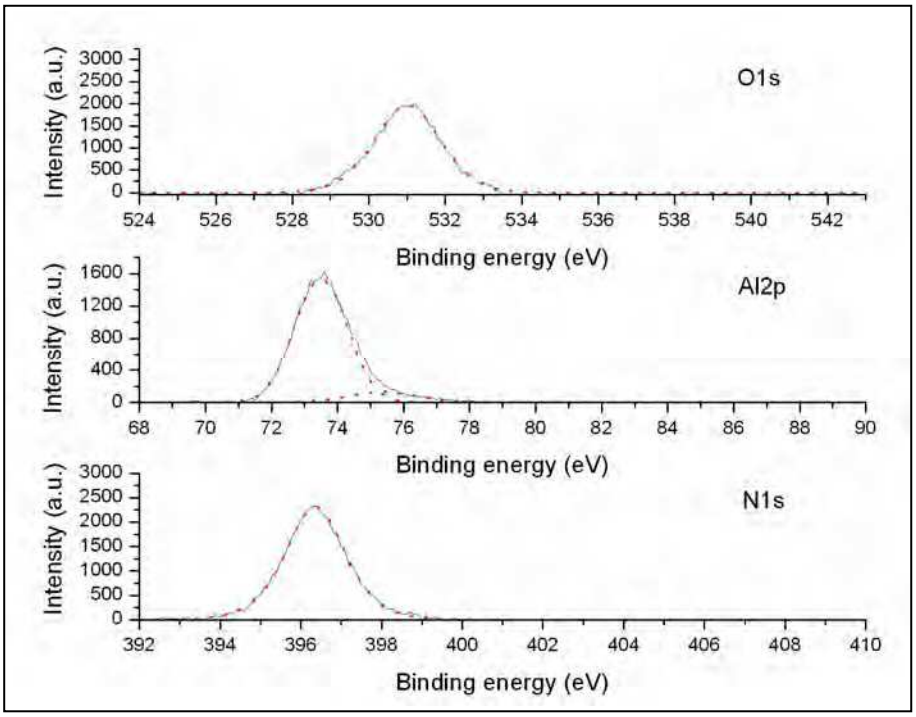

Fig. 7. O1s, Al2p and N1s XPS peaks acquired after surface cleaning on AlN_MR sample. The dotted red lines represent the peaks fitting the O1s peak.

The curves used for fitting the peaks, reported in Figure 7, represent a possible way to fit the XPS peaks found in the sample in order to understand how the atoms are bound in the film. The peaks used to fit the spectrum are those reported in literature, corresponding to Al-O and Al-N bonds. However, by using this method, the resulting percentage of Al-O bonds is too low (about 8%) if considering the oxygen concentration in the film (26.7 %). For this reason it is possible to assume that the film contains an AlO_xN_y phase which cannot be exactly estimated because a small variation of the position of each peak used for the fit of the main Al peak determines a high variation in the relative percentages of the different bonds.

The results obtained from the XPS analysis performed on AlN thin films deposited from a ceramic target confirm what already shown by EDS analysis: nitrogen was not detected in the films. XPS spectra for AlN_CN and AlN_CR are shown in Figure 8 and Figure 9. In spite of the absence of nitrogen in the films, a deeper investigation on the spectra can lead to interesting information. There is, in fact, a slight difference in the two spectra.

Although an accurate estimation of the concentration is not allowed because of the low and noisy signal obtained in the spectral region corresponding to the nitrogen peak position, a faint peak can be distinguished in Figure 9 at binding energies around 397.5 eV, the typical binding energy at which the N1s peak is centered when nitrogen is bound to aluminum (Manova et al., 1998).

The collection of the nitrogen peak in sample AlN_CR allows to assert that the presence of nitrogen gas during the sputtering process is necessary in order to include nitrogen in the film. Nonetheless the amount of gas used during the growth process was too low, and that is the reason why only noise was acquired in the spectral region of the N1s peak.

Sample name	C atomic concentration (%)	N atomic concentration (%)	O atomic concentration (%)	Al atomic concentration (%)
AlN_MR	-	34.2	26.7	39
AlN_CN	-	0.03	66.91	33.06
AlN_CR	0.28	0.35	65.73	33.63

Table 7. Atomic concentrations obtained by fitting the C1s, N1s, O1s and Al2p peaks from the XPS spectra of AlN thin films

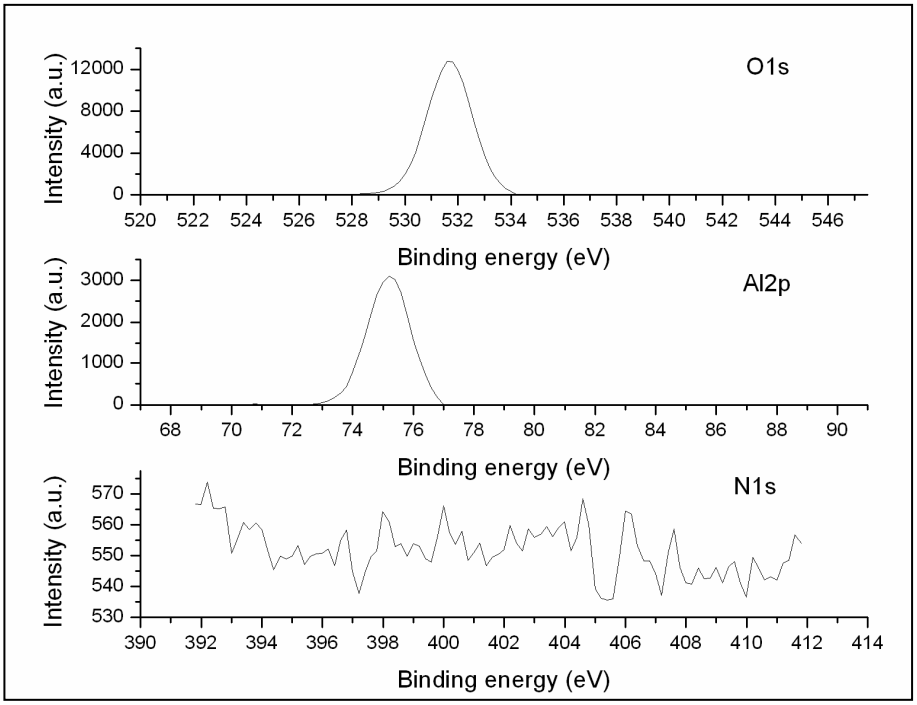

Fig. 8. O1s, Al2p and N1s XPS peaks acquired after surface cleaning on AlN_CN sample

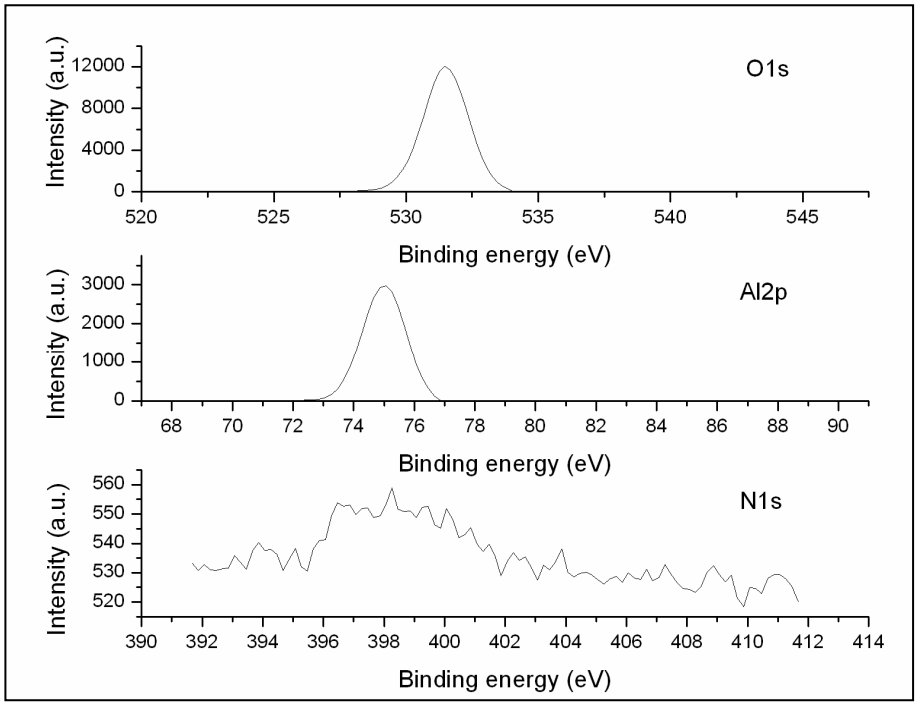

Fig. 9. O1s, Al2p and N1s XPS peaks acquired after surface cleaning on AlN_CR sample

4.2.3 XRD analysis on AlN thin films

Without the support of the EDS and XPS analyses on the AlN thin films grown from metal and ceramic targets, the interpretation of the XRD patterns would be more complicated. It is not usual in sputtering processes to obtain materials not maintaining a stoichiometry similar to that of the material source. However, for some classes of compounds, such as nitrides, this phenomenon is more frequent because one of the constituting elements is volatile and is less reactive than oxygen. In vacuum chambers used for the growth of both oxides and nitrides the chances of introducing contaminations in the films are numerous because of the residual oxygen trapped at the chamber walls. Moreover the residual humidity in the chamber containing oxygen is also responsible for the presence of oxide phases in the thin films. With such a low amount of nitrogen in the chamber, the compensation for the loss of nitrogen during the film growth cannot be achieved.

XRD patterns for all the analyzed samples are shown in Figure 10, while the peak positions are reported in Table 8. On the basis of the results discussed above, it was obvious that any peak acquired by XRD analysis of AlN_CN and AlN_CR samples should be identified as a peak corresponding to crystalline alumina phase and not to AlN crystalline phases. The chances that the 0.3 % of nitrogen found by fitting the XPS peak might form a crystalline phase with aluminum that could be detected by XRD are in fact very low. For this reason, all the diffraction peaks of the samples deposited from ceramic target were compared with the database peaks of Al_2O_3. The only detectable peak (with the exception of the peaks

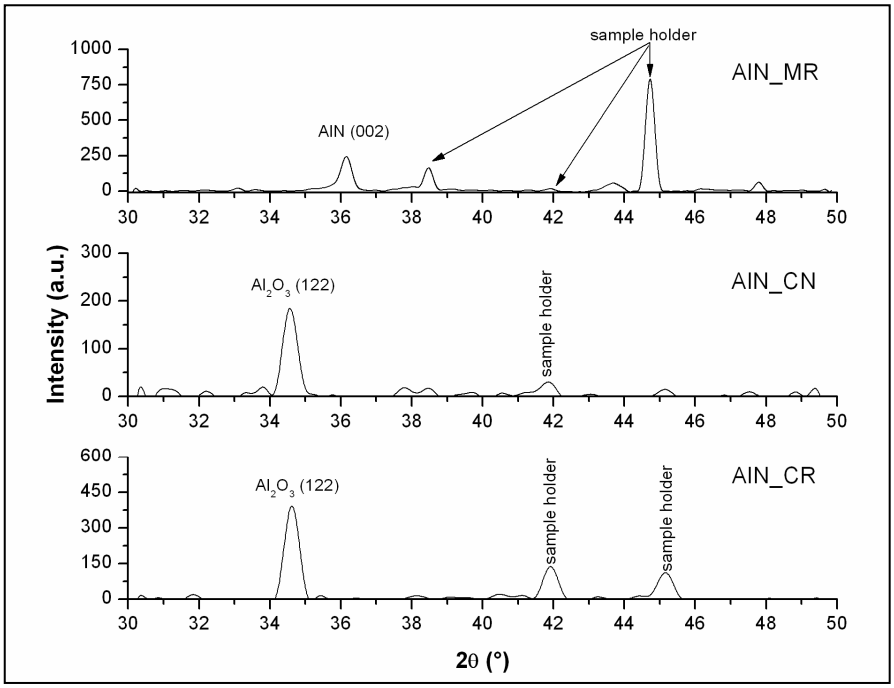

Fig. 10. XRD patterns of AlN thin films

Sample name	Peak position (2θ)	
	AlN [002]	Al_2O_3 [122]
	(degrees)	(degrees)
Database (JCPDS, 1998b)	35.981±0.001	34.734±0.001
AlN_MR	36.15±0.02	-
AlN_CN	-	34.57±0.02
AlN_CR	-	34.62±0.02

Table 8. Position of the peaks detected during XRD analysis performed on AlN thin film

produced by the sample holder) and present in the spectra of both films, was attributed to the [122] orientation of crystalline alumina.

For sample Al_MR instead, a peak corresponding to the [002] orientation of crystalline AlN was detected. In the view of obtaining films with good piezoelectric properties this is a good result since the highest piezoelectric coefficient for AlN is found to be along the *c*-axis orientation. There is certainly a problem of oxygen contamination that has to be solved in order to minimize the amorphous AlO_xN_y phase and increase the quality of the material but it is strictly related to technological issues.

The correct interpretation of XRD patterns was possible only on the basis of the results obtained from EDS and XPS analysis. If considering only the growth conditions of the films,

the attribution of the sole detected peak to an alumina phase could not be so obvious. The assignment of the detected peak to an aluminium oxide nitride compound, for example, would have been straightforward. From the database, in fact, it is possible to find a peak corresponding to the [103] orientation of such a compound centered at 34.357° (JCPDS, 1998c), very close to the position of the peaks detected in the AlN_CN and AlN_CR samples. On the basis of the sole experimental set up the material could be logically thought as a nitride. The misinterpretation of the XRD results was avoided just because of the availability of additional data related to the film composition.

5. Conclusions

Aluminum nitride and zinc oxide thin films were grown by the RF magnetron sputtering technique. Three methods were used for depositing each of the two materials, involving the use of different material sources and gas mixtures. Both materials are piezoelectric and this property is guaranteed and maximized when the material has certain characteristics. The analysis based on X-ray spectroscopy of all the samples was aimed at the comparison of the quality of films grown with the different methods and to select the most effective. In addition, the characterization results were used to underline the differences in the technological processes used for the growth of different classes of materials (oxides and nitrides). In particular, the growth of nitrides is characterized by issues due to the nature of the material itself, especially for what concerns nitrogen which is a volatile element and is characterized by a higher ionization energy than oxygen, that make it less reactive, lowering the possibilities to include such element in the films.

With reference to the growth of zinc oxide thin films, the approach that guaranteed a good stoichiometry and at the same time favored the growth along the *c*-axis was that characterized by the use of a ceramic target in the presence of a gas mixture containing Ar and O_2. Although a slight excess of zinc with respect to the right stoichiometry was detected, the film was mainly [002]-oriented. The future optimization of the parameters will be aimed at the growth of fully [002]-oriented ZnO thin films in order to maximize the piezoelectric coefficient of the material.

An aluminum nitride thin film was successfully grown only by reactive sputtering in nitrogen atmosphere. The growth from ceramic target led instead to the growth of aluminum oxide as confirmed by the X-ray spectroscopy analysis performed on the samples. The amount of nitrogen required for its inclusion in the film is higher than that used for the growth of the oxide samples. In spite of the not fully positive results related to the presence of nitrogen in the films, these experiments were useful for assessing the great importance of the combination of results coming from different analysis. The correct interpretation of XRD patterns of samples grown from ceramic target was possible only because of the presence of EDS and XPS data.

6. References

Akiyama, M., Morofuji, Y., Kamohara, T., Nishikubo, K., Tsubai, M., Fukuda, O. & Ueno, N. (2006). Flexible piezoelectric pressure sensors using oriented aluminum nitride thin films prepared on polyethylene terephthalate films. *Journal of Applied Physics*, Vol. 100, No. 11, pp. 114318

Avalle, L., Santos, E., Leiva, E. & Macagno, V. A. (1992). Characterization of TiO_2 films modified by platinum doping. *Thin Solid Films*, Vol. 219, No. 1-2, pp. 7-17, ISSN 0040-6090

Berg, S. & Nyberg, T. (2005). Fundamental understanding and modeling of reactive sputtering processes. *Thin Solid Films*, Vol. 476, No. 2, pp. 215-230, ISSN 0040-6090

Bohne, W., Röhrich, J., Schöpke, A., Selle, B., Sieber, I., Fuhs, W., del Prado, Á., San Andrés, E., Mártil, I. & González-Díaz, G. (2004). Compositional analysis of thin SiO_xN_y:H films by heavy-ion ERDA, standard RBS, EDX and AES: a comparison. *Nuclear Instruments and Methods in Physics Research Section B: Beam Interactions with Materials and Atoms*, Vol. 217, No. 2, pp. 237-245, ISSN 0168-583X

Briggs, D. & Seah, M. P. (1983a). Practical Surface Analysis: Auger and X-ray photoelectron spectroscopy., Briggs, D. & Seah, M. P., pp. 112, John Wiley & Sons, Chichester

Briggs, D. & Seah, M. P. (1983b). Practical Surface Analysis: Auger and X-ray photoelectron spectroscopy., Briggs, D. & Seah, M. P., pp. 51, John Wiley & Sons, Chichester

Briggs, D. & Seah, M. P. (1983c). Practical Surface Analysis: Auger and X-ray photoelectron spectroscopy., Briggs, D. & Seah, M. P., pp. 69, John Wiley & Sons, Chichester

Briggs, D. & Seah, M. P. (1983d). Practical Surface Analysis: Auger and X-ray photoelectron spectroscopy., Briggs, D. & Seah, M. P., pp. 120, John Wiley & Sons, Chichester

Chen, M., Wang, X., Yu, Y. H., Pei, Z. L., Bai, X. D., Sun, C., Huang, R. F. & Wen, L. S. (2000). X-ray photoelectron spectroscopy and auger electron spectroscopy studies of Al-doped ZnO films. *Applied Surface Science*, Vol. 158, No. 1-2, pp. 134-140, ISSN 0169-4332

Cheng, H., Sun, Y., Zhang, J. X., Zhang, Y. B., Yuan, S. & Hing, P. (2003). AlN films deposited under various nitrogen concentrations by RF reactive sputtering. *Journal of Crystal Growth*, Vol. 254, No. 1-2, pp. 46-54, ISSN 0022-0248

Cullity, B. D. (1956a). Elements of x-ray diffraction, Cullity, B. D., pp. 92, Addison-Wesley Publishing Company, Reading, Massachusetts, USA

Cullity, B. D. (1956b). Elements of x-ray diffraction, Cullity, B. D., pp. 189-190, Addison-Wesley Publishing Company, Reading, Massachusetts, USA

Cullity, B. D. (1956c). Elements of x-ray diffraction, Cullity, B. D., pp. 281, Addison-Wesley Publishing Company, Reading, Massachusetts, USA

Cullity, B. D. (1956d). Elements of x-ray diffraction, Cullity, B. D., pp. 102, Addison-Wesley Publishing Company, Reading, Massachusetts, USA

Du, X.-h., Wang, Q.-M., Belegundu, U., Bhalla, A. & Uchino, K. (1999). Crystal orientation dependence of piezoelectric properties of single crystal barium titanate. *Materials Letters*, Vol. 40, No. 3, pp. 109-113, ISSN 0167-577X

Ferblantier, G., Mailly, F., Al Asmar, R., Foucaran, A. & Pascal-Delannoy, F. (2005). Deposition of zinc oxide thin films for application in bulk acoustic wave resonator. *Sensors and Actuators A: Physical*, Vol. 122, No. 2, pp. 184-188, ISSN 0924-4247

Gautschi, G. (2002). *Piezoelectric Sensorics* (1st edition), Springer-Verlag Berlin Heidelberg New York, ISBN 978-3-540-42259-4, Germany.

Goldstein, J., Newbury, D.E., Joy, D.C., Lyman, C.E., Echlin, P., Lifshin, E., Sawyer, L.C. & Michael, J.R. (2003a). Scanning Electron Microscopy and X-ray Microanalysis, Goldstein, J., pp. 297, Springer Science + Business Media, ISBN 0306472929, New York, USA

Goldstein, J., Newbury, D.E., Joy, D.C., Lyman, C.E., Echlin, P., Lifshin, E., Sawyer, L.C. & Michael, J.R. (2003b). Scanning Electron Microscopy and X-ray Microanalysis, Goldstein, J., pp. 271, Springer Science + Business Media, ISBN 0306472929, New York, USA

Goldstein, J., Newbury, D.E., Joy, D.C., Lyman, C.E., Echlin, P., Lifshin, E., Sawyer, L.C. & Michael, J.R. (2003c). Scanning Electron Microscopy and X-ray Microanalysis, Goldstein, J., pp. 275, Springer Science + Business Media, ISBN 0306472929, New York, USA

Goldstein, J., Newbury, D.E., Joy, D.C., Lyman, C.E., Echlin, P., Lifshin, E., Sawyer, L.C. & Michael, J.R. (2003d). Scanning Electron Microscopy and X-ray Microanalysis, Goldstein, J., pp. 282, Springer Science + Business Media, ISBN 0306472929, New York, USA

Goldstein, J., Newbury, D.E., Joy, D.C., Lyman, C.E., Echlin, P., Lifshin, E., Sawyer, L.C. & Michael, J.R. (2003e). Scanning Electron Microscopy and X-ray Microanalysis, Goldstein, J., pp. 286-288, Springer Science + Business Media, ISBN 0306472929, New York, USA

Goldstein, J., Newbury, D.E., Joy, D.C., Lyman, C.E., Echlin, P., Lifshin, E., Sawyer, L.C. & Michael, J.R. (2003f). Scanning Electron Microscopy and X-ray Microanalysis, Goldstein, J., pp. 349, Springer Science + Business Media, ISBN 0306472929, New York, USA

Haber, J., Stoch, J. & Ungier, L. (1976). X-ray photoelectron spectra of oxygen in oxides of Co, Ni, Fe and Zn. *Journal of Electron Spectroscopy and Related Phenomena*, Vol. 9, No. 5, pp. 459-467, ISSN 0368-2048

Hammer, M., Monty, C., Endriss, A. & Hoffmann, M. J. (1998). Correlation between Surface Texture and Chemical Composition in Undoped, Hard, and Soft Piezoelectric PZT Ceramics. *Journal of the American Ceramic Society*, Vol. 81, No. 3, pp. 721-724, ISSN 1551-2916

Hirata, S., Okamoto, K., Inoue, S., Kim, T. W., Ohta, J., Fujioka, H. & Oshima, M. (2007). Epitaxial growth of AlN films on single-crystalline Ta substrates. *Journal of Solid State Chemistry*, Vol. 180, No. 8, pp. 2335-2339, ISSN 0022-4596

Huang, C.-L., Tay, K.-W. & Wu, L. (2005). Fabrication and performance analysis of film bulk acoustic wave resonators. *Materials Letters*, Vol. 59, No. 8-9, pp. 1012-1016, ISSN 0167-577X

Joint Committee on Powder Diffraction Standards (JCPDS) database—International Center for Diffraction Data (1998a) PCPDFWIN v.2.01. The JCPDS card number of ZnO is 89-1397

Joint Committee on Powder Diffraction Standards (JCPDS) database—International Center for Diffraction Data (1998b) PCPDFWIN v.2.01. The JCPDS card number of AlN is 89-3446 and JCPDS card number of Al2O3 is 88-0107

Joint Committee on Powder Diffraction Standards (JCPDS) database—International Center for Diffraction Data (1998c) PCPDFWIN v.2.01. The JCPDS card number of aluminum oxide nitride is 48-1581

Kelly, P. J. & Arnell, R. D. (2000). Magnetron sputtering: a review of recent developments and applications. *Vacuum*, Vol. 56, No. 3, pp. 159-172, ISSN 0042-207X

Klein, J. C. & Hercules, D. M. (1983). Surface characterization of model Urushibara catalysts. *Journal of Catalysis*, Vol. 82, No. 2, pp. 424-441, ISSN 0021-9517

Lee, J. B., Kim, H. J., Kim, S. G., Hwang, C. S., Hong, S.-H., Shin, Y. H. & Lee, N. H. (2003). Deposition of ZnO thin films by magnetron sputtering for a film bulk acoustic resonator. *Thin Solid Films*, Vol. 435, No. 1-2, pp. 179-185, ISSN 0040-6090

Maniv, S. & Westwood, W. D. (1980). Oxidation of an aluminum magnetron sputtering target in Ar/O_2 mixtures. *Journal of Applied Physics*, Vol. 51, No. 1, pp. 718-725, ISSN 0021-8979

Manova, D., Dimitrova, V., Fukarek, W. & Karpuzov, D. (1998). Investigation of d.c.-reactive magnetron-sputtered AlN thin films by electron microprobe analysis, X-ray photoelectron spectroscopy and polarised infra-red reflection. *Surface and Coatings Technology*, Vol. 106, No. 2-3, pp. 205-208, ISSN 0257-8972

Muthukumar, S., Gorla, C. R., Emanetoglu, N. W., Liang, S. & Lu, Y. (2001). Control of morphology and orientation of ZnO thin films grown on SiO_2/Si substrates. *Journal of Crystal Growth*, Vol. 225, No. 2-4, pp. 197-201, ISSN 0022-0248

Penza, M., De Riccardis, M. F., Mirenghi, L., Tagliente, M. A. & Verona, E. (1995). Low temperature growth of r.f. reactively planar magnetron-sputtered AlN films. *Thin Solid Films*, Vol. 259, No. 2, pp. 154-162, ISSN 0040-6090

Ramam, K. & Chandramouli, K. (2011). Dielectric and piezoelectric properties of rare-earth gadolinium modified lead lanthanum zirconium niobium titanate ceramics. Ceramics International, Vol. 37, No. 3, pp. 979-984, ISSN 0272-8842

Ruffner, J. A., Clem, P. G., Tuttle, B. A., Dimos, D. & Gonzales, D. M. (1999). Effect of substrate composition on the piezoelectric response of reactively sputtered AlN thin films. *Thin Solid Films*, Vol. 354, No. 1-2, pp. 256-261, ISSN 0040-6090

Safi, I. (2000). Recent aspects concerning DC reactive magnetron sputtering of thin films: a review. *Surface and Coatings Technology*, Vol. 127, No. 2-3, pp. 203-218, ISSN 0257-8972

Sproul, W. D., Christie, D. J. & Carter, D. C. (2005). Control of reactive sputtering processes. *Thin Solid Films*, Vol. 491, No. 1-2, pp. 1-17, ISSN 0040-6090

Sundaram, K. B. & Khan, A. (1997). Characterization and optimization of zinc oxide films by r.f. magnetron sputtering. *Thin Solid Films*, Vol. 295, No. 1-2, pp. 87-91, ISSN 0040-6090

Waite, M. M. & Shah, S. I. (2007). Target poisoning during reactive sputtering of silicon with oxygen and nitrogen. *Materials Science and Engineering: B*, Vol. 140, No. 1-2, pp. 64-68, ISSN 0921-5107

Wasa, K., Kitabatake, M. & Adachi, H. (2004a). Sputtering systems, in: *Thin film materials technology-sputtering of compound materials*. K. Wasa, M. Kitabatake, H. Adachi, pp. 135, William Andrew Publishing, Norwick, NY/Springer-Verlag, ISBN 3-540-21118-7, Heidelberg, Germany

Wasa, K., Kitabatake, M. & Adachi, H. (2004b). Sputtering systems, in: *Thin film materials technology-sputtering of compound materials*. K. Wasa, M. Kitabatake, H. Adachi, pp. 139, William Andrew Publishing, Norwick, NY/Springer-Verlag, ISBN 3-540-21118-7, Heidelberg, Germany

Wright, R. V., Hakemi, G. & Kirby, P. B. (2011). Integration of thin film bulk acoustic resonators onto flexible liquid crystal polymer substrates. *Microelectronic Engineering*, Vol. 88, No. 6, pp. 1006-1009, ISSN 0167-9317

Xu, X.-H., Wu, H.-S., Zhang, C.-J. & Jin, Z.-H. (2001). Morphological properties of AlN piezoelectric thin films deposited by DC reactive magnetron sputtering. *Thin Solid Films*, Vol. 388, No. 1-2, pp. 62-67, ISSN 0040-6090

Yan, Z., Zhou, X. Y., Pang, G. K. H., Zhang, T., Liu, W. L., Cheng, J. G., Song, Z. T., Feng, S. L., Lai, L. H., Chen, J. Z. & Wang, Y. (2007). ZnO-based film bulk acoustic resonator for high sensitivity biosensor applications. *Applied Physics Letters*, Vol. 90, No. 14, pp. 143503

Yue, W. & Yi-jian, J. (2003). Crystal orientation dependence of piezoelectric properties in $LiNbO_3$ and $LiTaO_3$. *Optical Materials*, Vol. 23, No. 1-2, pp. 403-408, ISSN 0925-3467

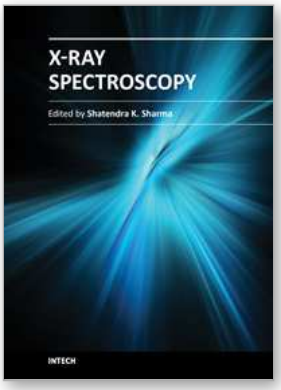

X-Ray Spectroscopy

Edited by Dr. Shatendra K Sharma

ISBN 978-953-307-967-7
Hard cover, 280 pages
Publisher InTech
Published online 01, February, 2012
Published in print edition February, 2012

The x-ray is the only invention that became a regular diagnostic tool in hospitals within a week of its first observation by Roentgen in 1895. Even today, x-rays are a great characterization tool at the hands of scientists working in almost every field, such as medicine, physics, material science, space science, chemistry, archeology, and metallurgy. With vast existing applications of x-rays, it is even more surprising that every day people are finding new applications of x-rays or refining the existing techniques. This book consists of selected chapters on the recent applications of x-ray spectroscopy that are of great interest to the scientists and engineers working in the fields of material science, physics, chemistry, astrophysics, astrochemistry, instrumentation, and techniques of x-ray based characterization. The chapters have been grouped into two major sections based upon the techniques and applications. The book covers some basic principles of satellite x-rays as characterization tools for chemical properties and the physics of detectors and x-ray spectrometer. The techniques like EDXRF, WDXRF, EPMA, satellites, micro-beam analysis, particle induced XRF, and matrix effects are discussed. The characterization of thin films and ceramic materials using x-rays is also covered.

InTech Europe
University Campus STeP Ri
Slavka Krautzeka 83/A
51000 Rijeka, Croatia
Phone: +385 (51) 770 447
Fax: +385 (51) 686 166
www.intechopen.com

InTech China
Unit 405, Office Block, Hotel Equatorial Shanghai
No.65, Yan An Road (West), Shanghai, 200040, China
中国上海市延安西路65号上海国际贵都大饭店办公楼405单元
Phone: +86-21-62489820
Fax: +86-21-62489821